08/28/2015
TD-15-018

LARP MQXFSM1 (Mirror) Magnet Test Summary

G. Chlachidze, S. Stoynev, G. Ambrosio, M. Anerella, N. Andreev, R. Bossert, R. Carcagno, D. Cheng, D. Dietderich, H. Felice, P. Ferracin, A. Ghosh, E. F. Holik, S. Izquierdo Bermudez, S. Krave, F. Lewis, F. Nobrega, I. Novitski, D. Orris, J. C. Perez, G.L. Sabbi, J. Schmalzle, C. Sylvester, M. Tartaglia, G. Velev, P. Wanderer, A.V. Zlobin

Content:

1. Introduction 2
2. Instrumentation 3
3. Quench Training 5
4. Ramp rate dependence 6
5. Temperature dependence 7
6. Holding Current tests 8
7. Splice Resistance Measurements 8
8. Inductance measurements 9
9. Strain Gauge Data 9
10. Quench Protection Studies 21
11. RRR measurements 25
12. Summary 25
Attachment I 27

1. Introduction

MQXFSM1 is the first 150-mm aperture Nb_3Sn quadrupole coil assembled and tested in a mirror structure by the US LHC Accelerator Research Program (LARP). This coil was developed within the joint efforts of the LARP and CERN for development of the inner triplet (low β) quadrupoles in the HiLumi-LHC project [1]. Previously LARP successfully fabricated and tested 90-mm (TQ, LQ) and 120-mm (HQ) aperture Nb_3Sn magnets [2-3]. In July 2012 the aperture of the triplet has been fixed to 150 mm diameter, based on a first estimate of the shielding necessary to cope with radiation damage and heat loads, and on the beam dynamics requirements.

1.5-m long coil in MQXFSM1 was made of 40-strand Rutherford cable with 0.85-mm Nb_3Sn strand based on the "Restack Rod Process" (RRP) of 108/127 sub-element design. Stainless Steel core was placed between the layers of the superconductor. The strand was manufactured by Oxford Instruments Superconducting Technology [4]. According to the specifications, the strand will have a critical current in the superconductor of 2450 A/mm^2 at 12 T and 4.2 K, and of 1280 A/mm^2 at 15 T and 4.2 K, the Cu/Sc ratio is 1.2. Some parameters of MQXFSM1 are shown in Table 1.

Various Nb_3Sn dipole and quadrupole coils were successfully tested in a mirror structure developed at Fermilab [5-6]. This approach allowed testing individual coils at the operating conditions similar to that of a real magnet, thus reducing the turnaround time of coil fabrication and evaluation, as well as material and labor costs.

The MQXFSM1 mirror magnet was installed into the VMTF dewar and it was electrically checked by May 1st, 2015. Cool down started on May 3rd and the VMTF dewar was filled with liquid helium next day (see Fig.1). Test was started on May 4th and was completed on May 22nd. Finally the mirror magnet has been removed from the VMTF dewar on June 3rd, 2015.

Table 1. MQXFSM1 Parameters

Parameters	**Units**	
RRP strand diameter	mm	0.85
Sub-element layout		108/127
Number of strands		40
Cable width	mm	18.094
Cable mid-thickness	mm	1.529
Keystone angle	degree	0.52
Cable twist pitch	mm	109
SSL at 4.5K/1.9K	kA	18.7/21.1
Peak field at 4.5K/1.9K	T	13.2/14.5

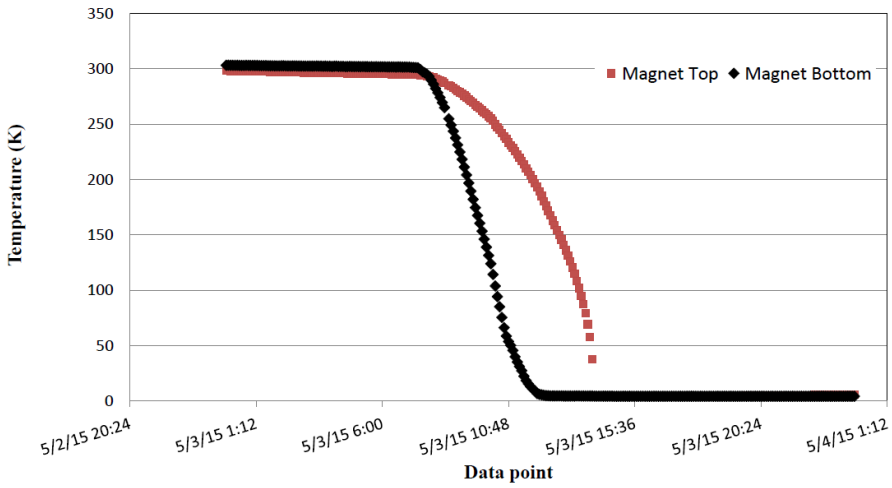

Fig. 1 MQXFSM1 cool down

2. Instrumentation

The mirror magnet was built using QXFS coil #2, magnet cross section is shown in Fig. 2. MQXFSM1 was equipped with 4 protection heater (PH) strips on the outer coil surface and 2 PH strips on the inner coil surface. The outer layer protection heaters were made of stainless steel (SS) with 6.4-6.5 Ohm resistance at room temperature, and the inner layer heaters were made of the copper cladded SS with 3.1 Ohm resistance (see Fig. 3). The inner layer heaters, as well as the outer layer heaters, located in the mid-plane and pole blocks were connected in series. The inner and outer coil heaters were connected to the different Heater Firing Units (HFU). In order to provide similar decay times for both groups of heaters (~ 32 ms) we used additional external 1.2 Ohm resistor connected in series to the inner layer heaters. Heater firing units were operated at 300-350 V and 19.2 mF of capacitance. Peak current in the individual heaters during the test varied from 45 to 52 A.

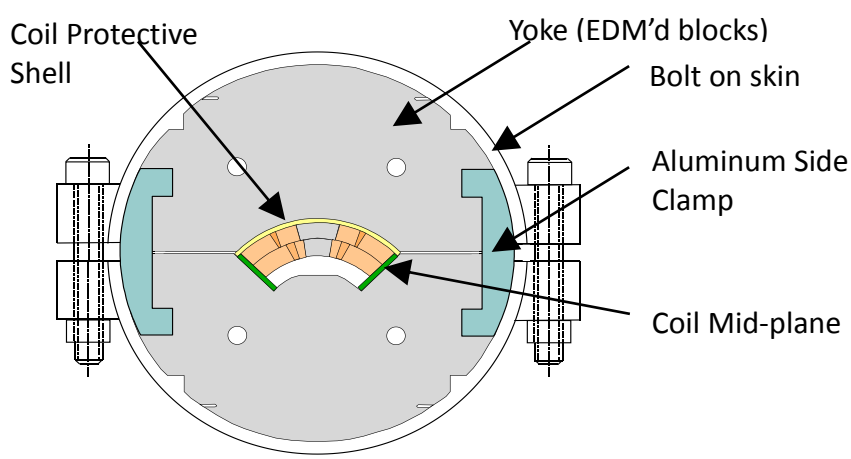

Fig. 2 MQXFSM1 mirror magnet cross section

Fig. 3 MQXFSM1 protection heaters on the outer (top) and inner (bottom) coils.

Voltage tap system in MQXFSM1 covers the inner and outer coil layers, pole turn, multi-turn and splice sections (see Fig. 4). There are 8 voltage taps on the inner layer and 8 voltage taps on the outer layer.

32 strain gauges (SG) were installed on the coil, bullets and skin for monitoring mechanical strain and calculating coil stresses during the magnet construction and testing. A set of full bridges was installed on inner titanium pole - one azimuthal bridge, one longitudinal bridge. 4 quarter bridges bonded to inside surface of inner coil, used during construction only.

In addition to the standard set of the dewar temperature sensors 2 additional resistive temperature devices (RTD) were mounted at top and bottom of the magnet outer skin (*Cernox cx50632* and *cx53825* sensors respectively), and were insulated from the surrounding gas to provide a better indication of the cold mass temperature during cool down and warm up.

Quench antenna (QA) was built using 5 printed circuit boards (PCB), each 4 cm long, distributed with different spacing along the whole length of the coil (see Fig. 5). These PCB were installed on a G10 strip and this strip mechanically was connected to the inner coil pole.

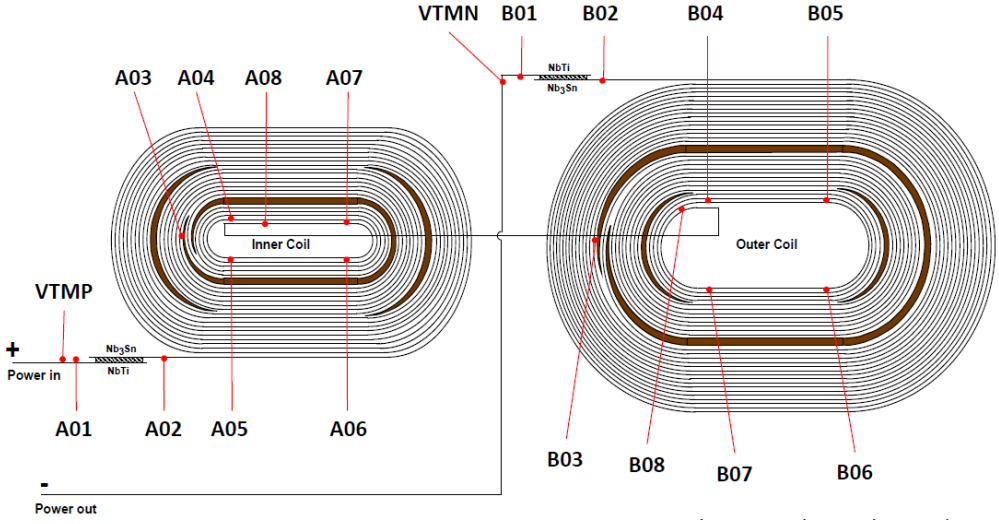

Fig. 4 Voltage tap locations for the inner (left) and outer (right) layers

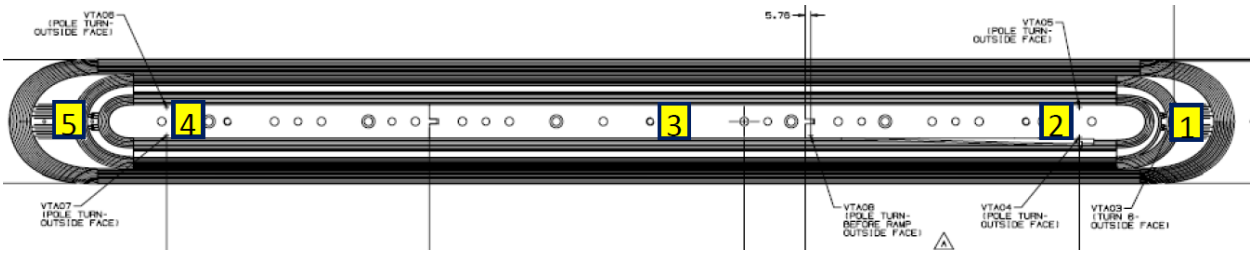

Fig. 5 Locations of the quench antenna segments

3. Quench Training

The magnet test program started with quench training at 20 A/s ramp rate at 1.9 K. After first few quenches training ramps were performed at mixed ramp rates: 50 A/s up to 12-14 kA and then continued to the quench at 20 A/s. The quench detection thresholds were set as in "default" configuration, since there was no need for further adjustment (see Attachment I). The first half-coil signal was formed by segments A01 to B08 (inner layer and the ramp between layers) and the second half – by segments B08 to B01 (outer layer).

The full quench training history is presented in Fig. 6. Training at 1.9 K started with a quench at 14814 A or 70.3% of SSL. Quench recovery was fast and we reached in average less than half an hour time interval between quenches thus managing 18 quenches the second day of the test. At the start training was very fast and we reached 82% of SSL in 5 quenches and 84.5% in 8 quenches.

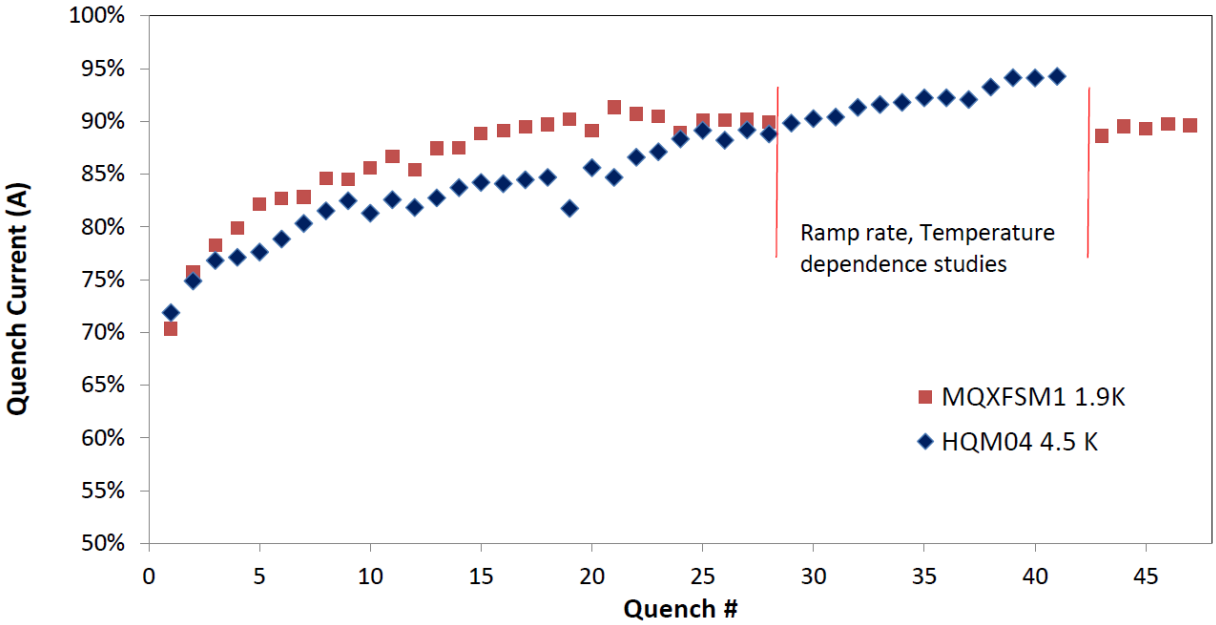

Fig. 6. MQXFSM1 quench history compared to HQM04 mirror magnet performance at 4.5 K

As Fig. 7 shows the initial quench locations were in both layers in high field segments around the pole (with one possible exception in multi-turn segment). Later on training continued slowly reaching a limit at ~19 kA or ~90% of the SSL at 1.9 K. The maximum quench current was 19239

A or 91.3% of SSL at 1.9K. Although two segments - A3-A4 and A4-A5 - were limiting the magnet performance, the time difference between them was within the uncertainty (noise) level and the pattern was similar in all of the quenches. Thus it was likely one and the same location on the LE side. This was confirmed by QA signals with a typical pattern of signals in both QA segments #1 and #2, arising at the same (within uncertainties) time. The signals from the voltage tap segments and QAs are consistent with a quench developing around the border of the two segments, close to the pole.

After more than five quenches with no further improvement in training it was decided to continue with ramp rate dependence study and other measurements according to the run plan.

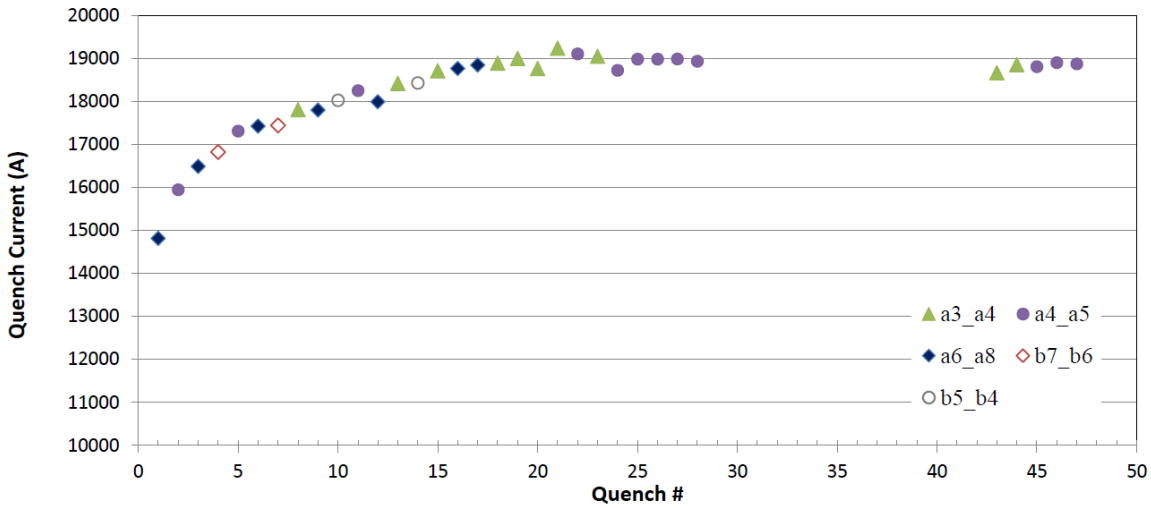

Fig. 7. MQXFSM1 quench locations. The separation after quench 28 indicates a couple of weeks of difference in time. The last 16 quenches likely happen at one and the same place as indicated in the text.

4. Ramp Rate Dependence

The ramp rate dependence study was performed at 1.9 K (see Fig. 8). Although the quench pattern in all ramp rate quenches were similar to the one in the latest training quenches, at high ramp rates above 300 A/s, the QA segment #4 was consistently detecting the quench. This observation suggests a quench location in the straight section, close to the RE but still in the pole turn. The same quench locations in the late training quenches and in all ramp rate quenches probably indicates that magnet reached its performance limits.

MQXFSM1 ramp rate dependence is consistent with the performance of magnet with a stainless steel core in the conductor. Compared to another mirror magnet (HQM04) quench current in MQXFSM1 is even less sensitive to the ramp rate change. Both mirror magnets show change of slope at around 200 A/s.

In addition, MQXFSM1 did not quench when ramped down from 18 kA flat top (85% of SSL at 1.9 K) at 300 A/s.

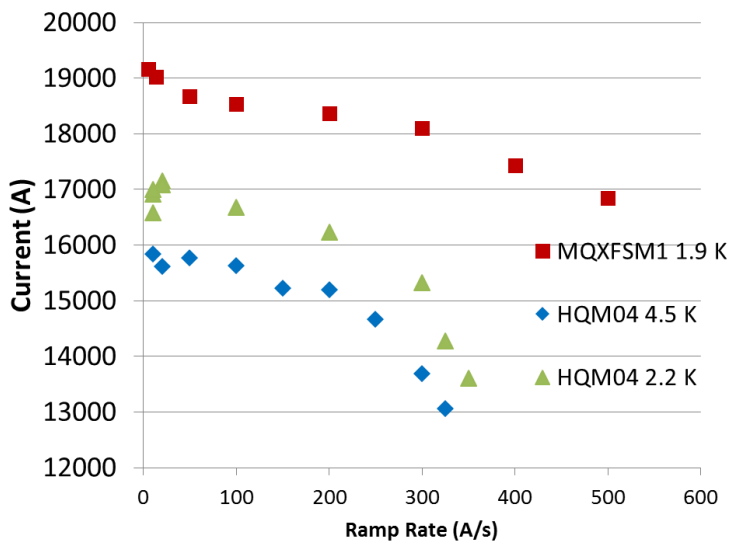

Fig. 8. MQXFSM1 ramp rate dependence compared to HQM04 mirror magnet

5. Temperature dependence

The temperature dependence of quench current is another demonstration of reached limits for the magnet performance. MQXFSM1 temperature dependence is shown in Fig. 9.

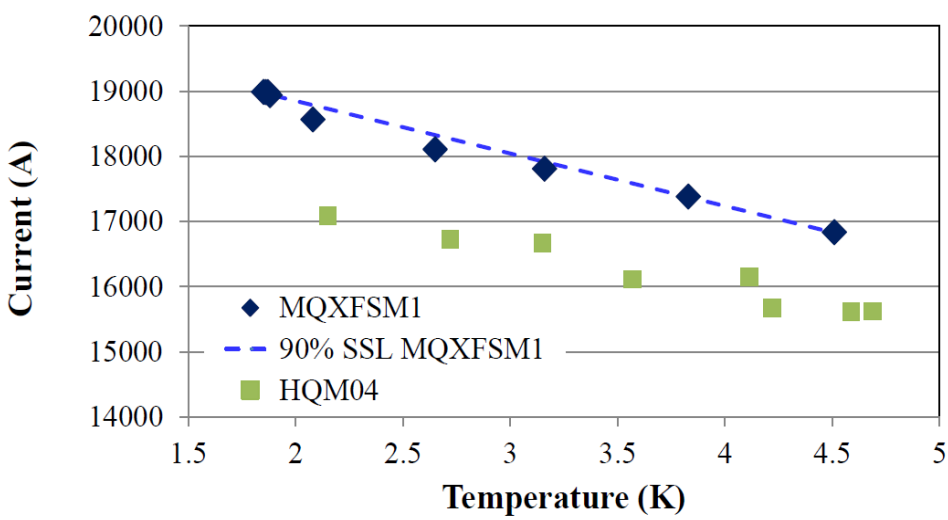

Fig. 9. Temperature dependence of the quench current in MQXFSM1

In contrast to the HQM04 mirror magnet MQXFSM1 shows little or no dependence of Iq/I_{SSL} on the temperature. Quenches at different temperatures originated from the same location between the A3-A4 and A4-A5 segments, similar to the training quenches. QA segments #1 and #2 were detecting first these quenches.

6. Holding current tests

These tests demonstrate capability of the magnet to hold high currents, close to or exceeding the nominal current value, for an extended time period.

Two attempts were made for holding the current for two hours. At 4.5K this test was performed at 16.5 kA (88% of SSL) and after two hours the current was ramped down. At 1.9 K test was performed at 17.8 kA (85% of SSL) and the current was held for two hours. However during ramp down at 20 A/s a quench developed at 17576 A. The quench origin was in the inner layer A3-A4 and A4-A5 segments, similar to the training quenches.

7. Splice resistance measurements

The MQXFSM1 mirror magnet has two Nb_3Sn to NbTi splices, one for the inner and one for the outer layer segments, A2-A1 and B2-B1 respectively. The splice resistence was measured by taking the VA-dependence at different currents up to 15 kA. At each current measurements were averaged, spikes or noise in readings were removed after a visual inspection of the data. The splice measurement data are presented in Fig. 10.

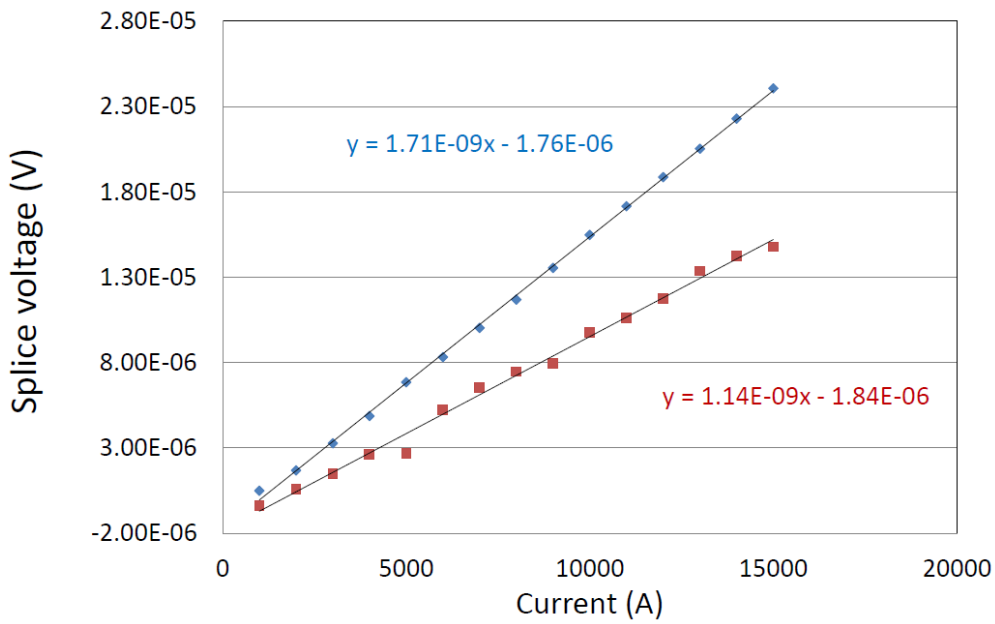

Fig. 10. Splice resistance measurements in MQXFSM1

As one can see from the plot there is a clear linear dependence of the voltage reading on the current. The resistances of the inner and outer layer splices are 1.7 nOhm and 1.1 nOhm, respectively. Although within the reasonable ranges, the inner layer splice resistance is at the high end of the range and can be regarded as high.

8. Inductance measurements

Inductance measurements were performed at 1.9 K. The magnet was ramped up to 16.5 kA and then ramped down at 200 A/s. The inductance as a function of current is shown in Fig. 11. The result is consistent with the room temperature measurement of 5.2 mH obtained with 20 Hz induced signal. Results were also confirmed at 4.5K with 200 and 300 A/s ramp rates (not shown in Fig. 11).

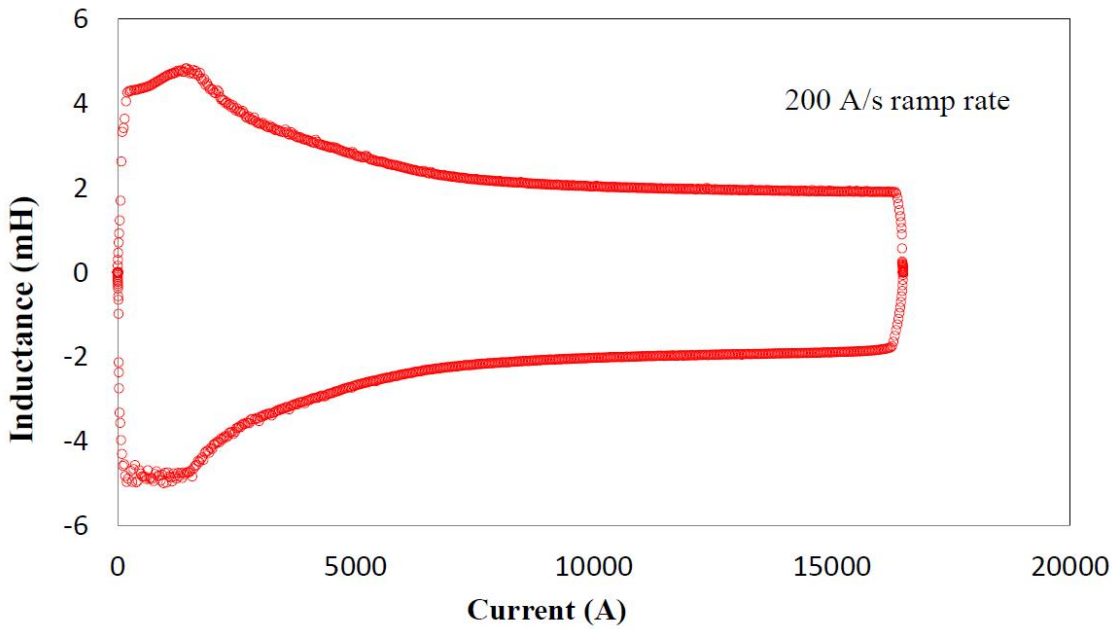

Fig. 11. MQXFSM1 inductance as a function of current

9. Strain gauge data

9.1. Strain gauge types and positions

Strain gauges were placed on the coil at various positions in MQXFSM1. Figure 12 shows the MQXFSM1 cross section with coil gauge positions shown. In the figure, T stands for “transition” side and NT stands for “non-transition” side. On the transition side, the pole turn makes the transition from the inner to the outer layer.

Figure 13 shows a picture of the strain gauges bonded to the inside of the coil. The system used is standard for short mirrors, consisting of:

- Two full bridges on the inner titanium pole, one azimuthal bridge, and one longitudinal bridge.

- Four quarter bridges, bonded to the inside surface of the inner coil, two near the midplane, and two near the pole.

Gauges bonded directly to the coil are used at room temperature during construction, and can give valuable insights into the preload during construction, particularly with respect to the relationship between pole and midplane values. They are not calibrated for cold measurements and are therefore disregarded during cold testing. A modulus of elasticity of 20 GPa is assumed for the coil when reading the coil gauges.

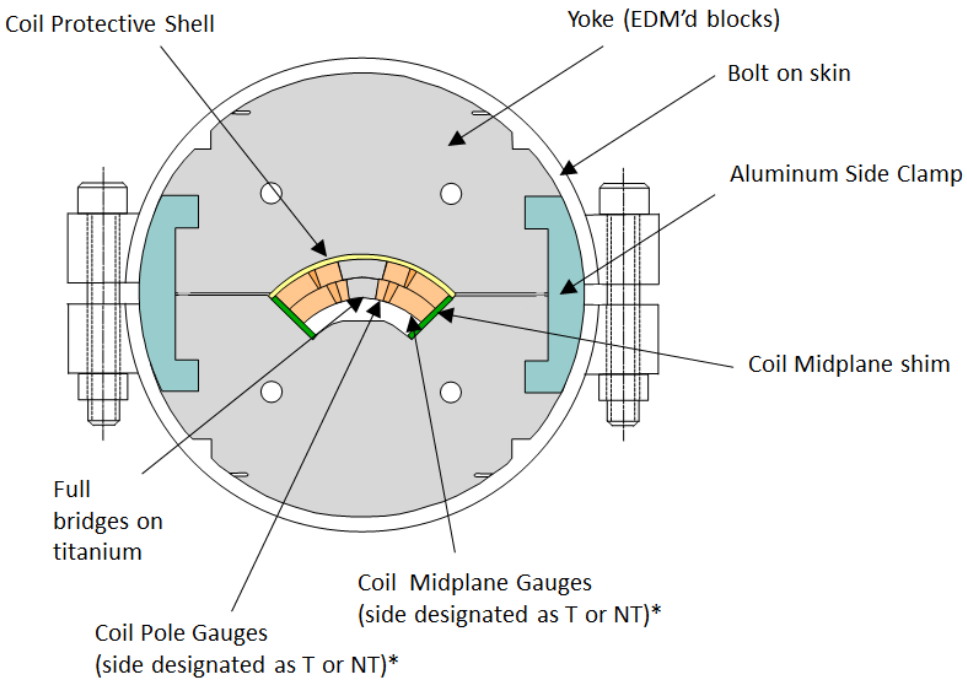

Fig. 12 Strain Gauge Positions

Strain gauges were also bonded to the end preload bolts (bullets). Similar to HQ mirrors, two preload bolts are placed on each end, each applying 7 kN (1500 pounds) of force from the 50mm thick end plate, for a total of 14 kN of force applied to each end at assembly. The preload bolts are positioned as shown in Fig. 14. A single half bridge is attached to each preload bolt. A gauge for temperature compensation is attached to a separate steel pin, and placed into a hole in the end plate. A bolt with strain gauges attached, along with a bullet temperature compensator is shown in Fig. 15.

An array of gauges (quarter bridges) were also bonded to the stainless steel shell, aligned in the azimuthal direction at positions of 60 and 90 degrees from the end plane, at two longitudinal positions, as shown in Fig. 16. Gauges bonded to the shell were read but were not analyzed, and are not reported here.

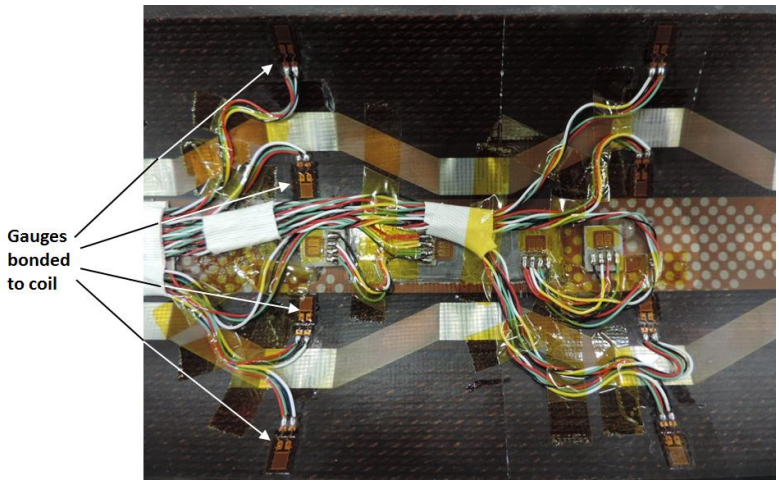

Fig. 13 Strain Gauges on coil MQXFSM1

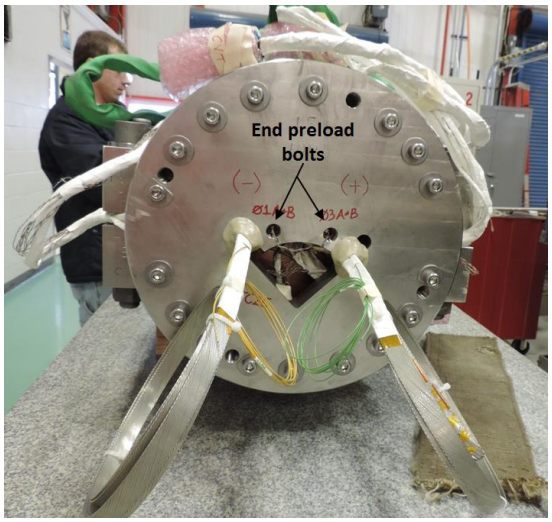

Fig. 14 Lead End view of MQXFSM1

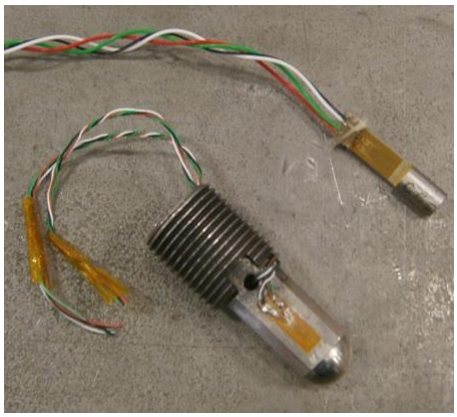

Fig. 15 Preload Bolt and Temperature Compensator

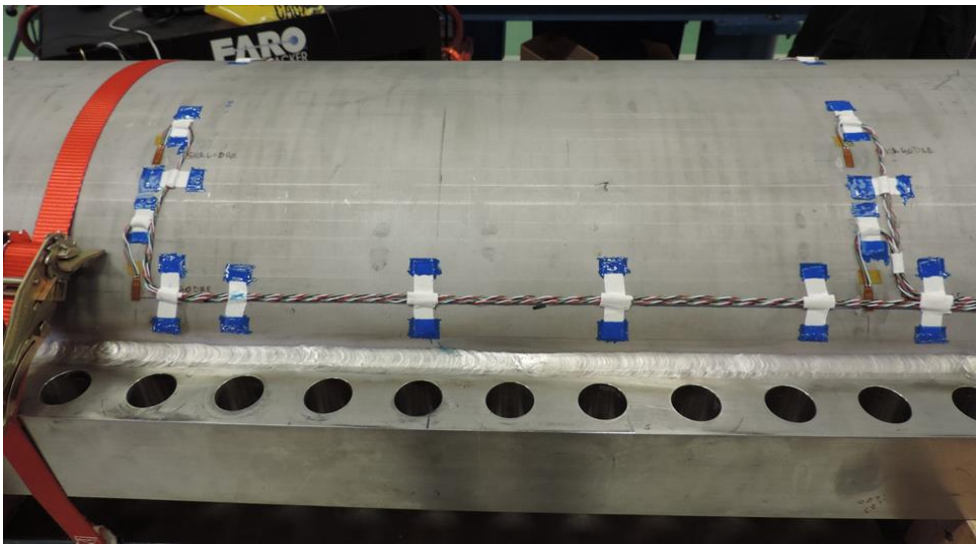

Fig. 16 Strain gauges on Shell

9.2. Finite Element Analysis

For reference, FEA for QXFSM1 is shown in Figures 17-19, at 300K, 4K without current, and 4K at 18 kA. Note that at quench current, the azimuthal Lorentz forces in the mirror are 30% lower than in the quadrupole model. Therefore lower coil pre-stress is needed.

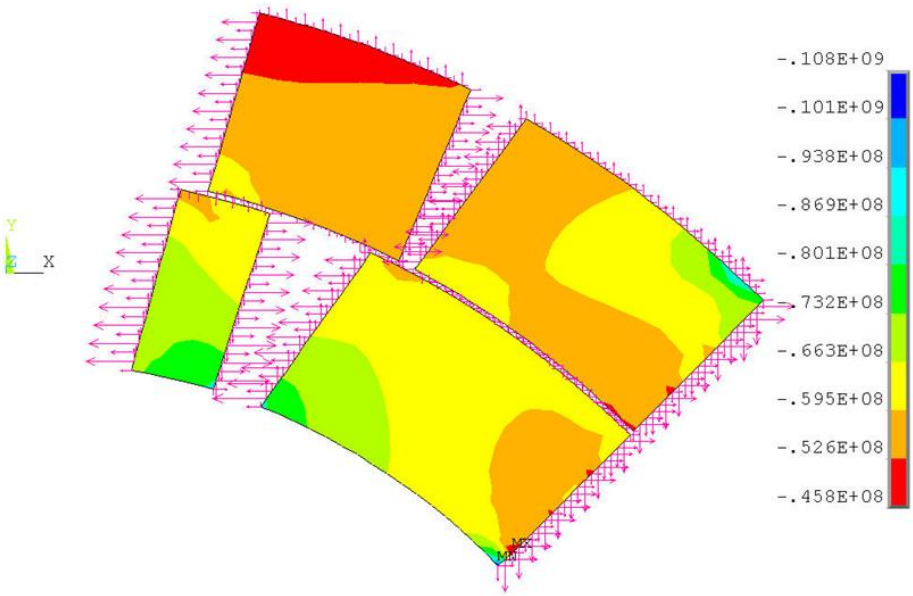

Fig. 17 FEA at 300K (units in Pa)

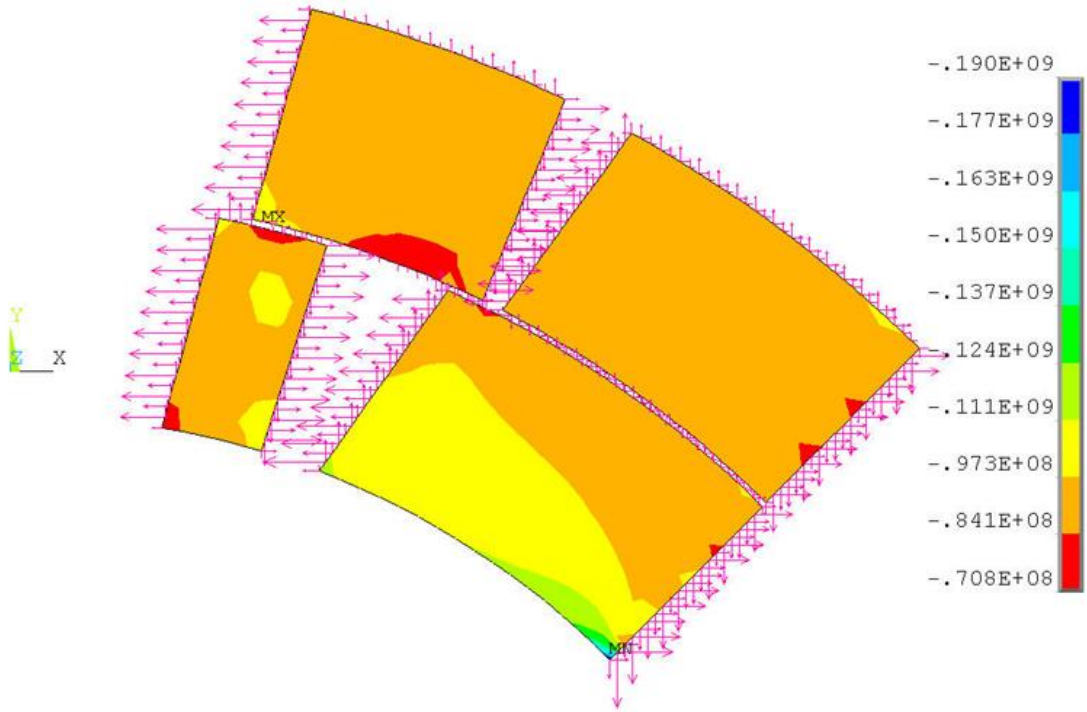

Fig. 18 FEA at 4K 0A (units in Pa)

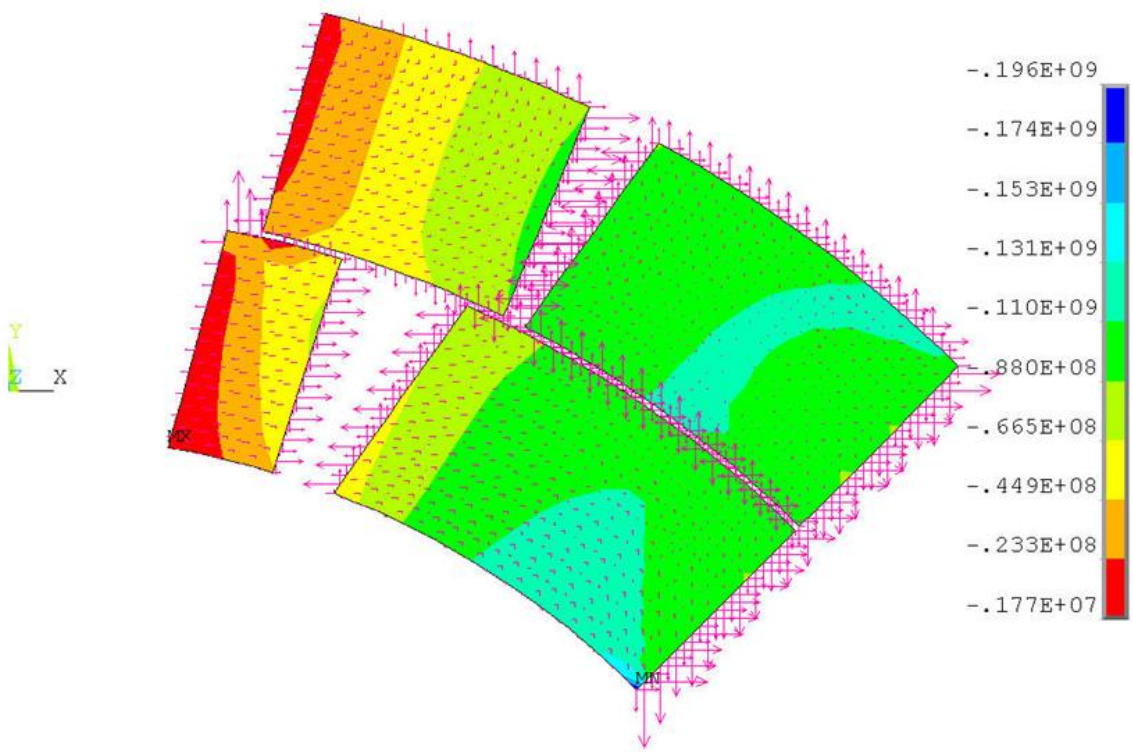

Fig. 19 FEA at 4K and 18 kA (units in Pa)

9.3. Strain gauge readings

Figures 20 through 24 show the assembly steps during construction, and the azimuthal and longitudinal preload readings from the full bridges bonded to the titanium. Preload in MPa is shown for the azimuthal bridges, while µS is given for the longitudinal bridges. Both the expected and actual preload are shown (expected in black, and actual in red).

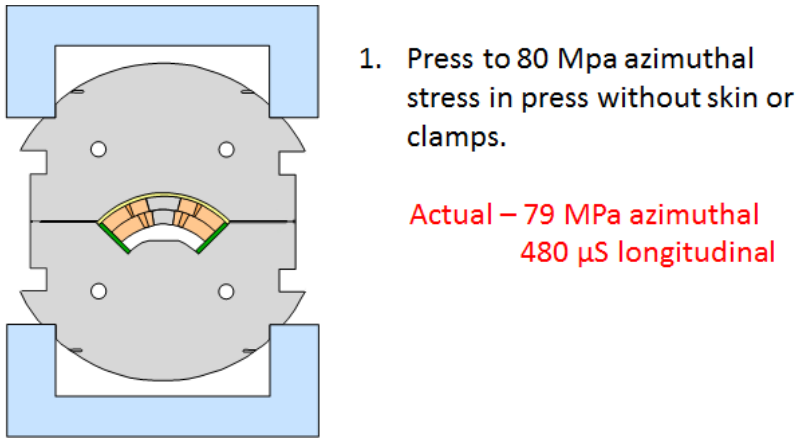

Fig. 20 Initial Pressing

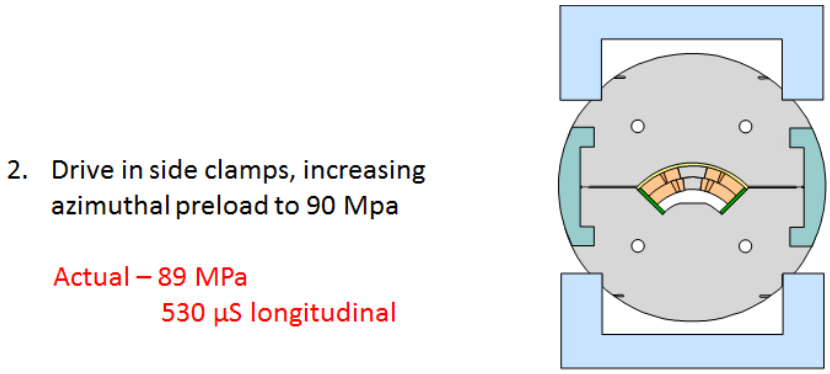

Fig. 21 with Side Clamps Installed, and Hydraulic Pressure Applied

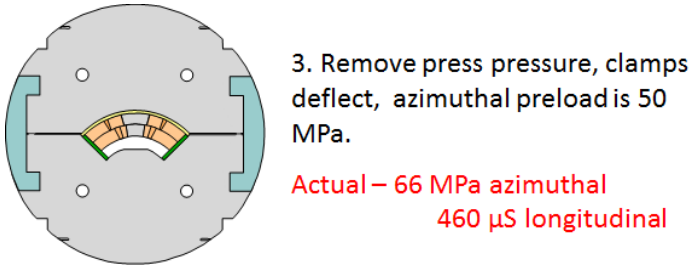

Fig. 22 with End Clamps Installed, and Hydraulic Pressure Removed

4. Install skin, return to press, press to azimuthal preload of 90 MPa.

Actual – 89 MPa azimuthal
310 µS longitudinal

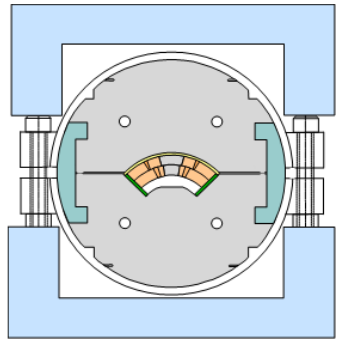

Fig. 23 with Shell (Skin) Installed, and Hydraulic Pressure Applied

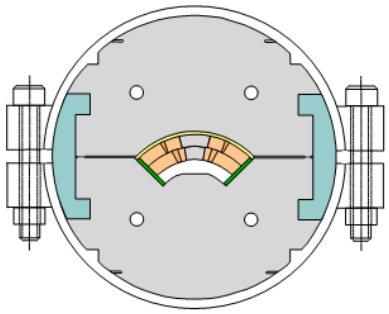

5. Bolt skin and release press. Final average azimuthal coil preload of 70 MPa.

Actual – 77 MPa azimuthal
270 µS longitudinal

Fig. 24 with Bolts Tightened, and Hydraulic Pressure Removed

Azimuthal and longitudinal (axial) full bridges were read during cooldown and excitation. Azimuthal bridges show a large positive change in strain with cooldown, with the 4K readings showing positive numbers, as if the coil is in tension, as shown in Fig. 25. Nevertheless, the strain continues to move further into the positive direction (by about 50 MPa) during excitation, as shown in Figures 26 and 27, indicating that preload remains after cooldown. This behavior has been observed in some previous mirrors, and is possibly due to bending of the coil (becoming more convex).

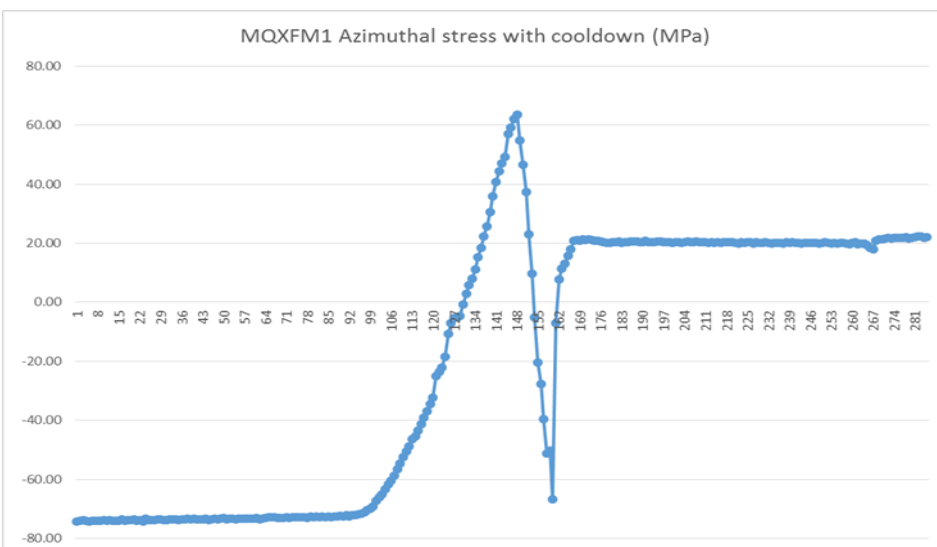

Fig. 25 Azimuthal Stress with Cooldown

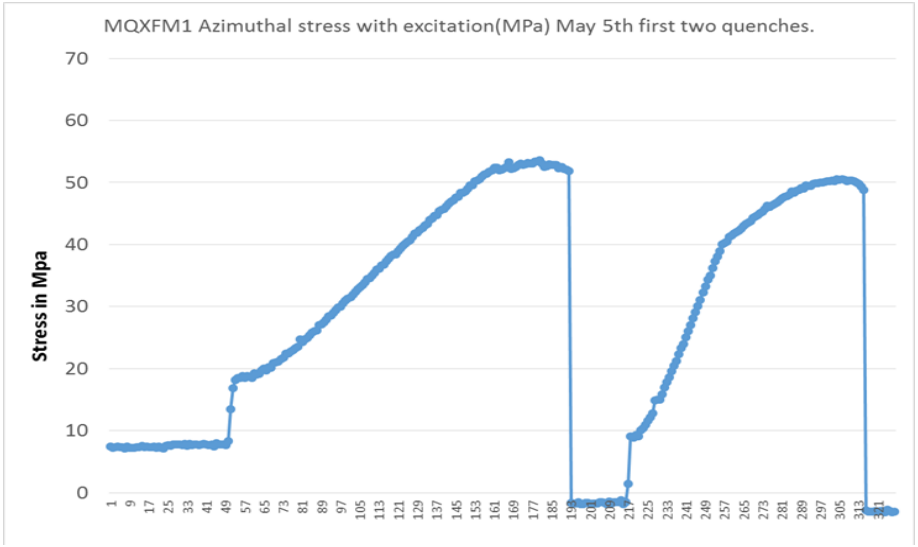

Fig. 26 Azimuthal Stress First Two Quenches

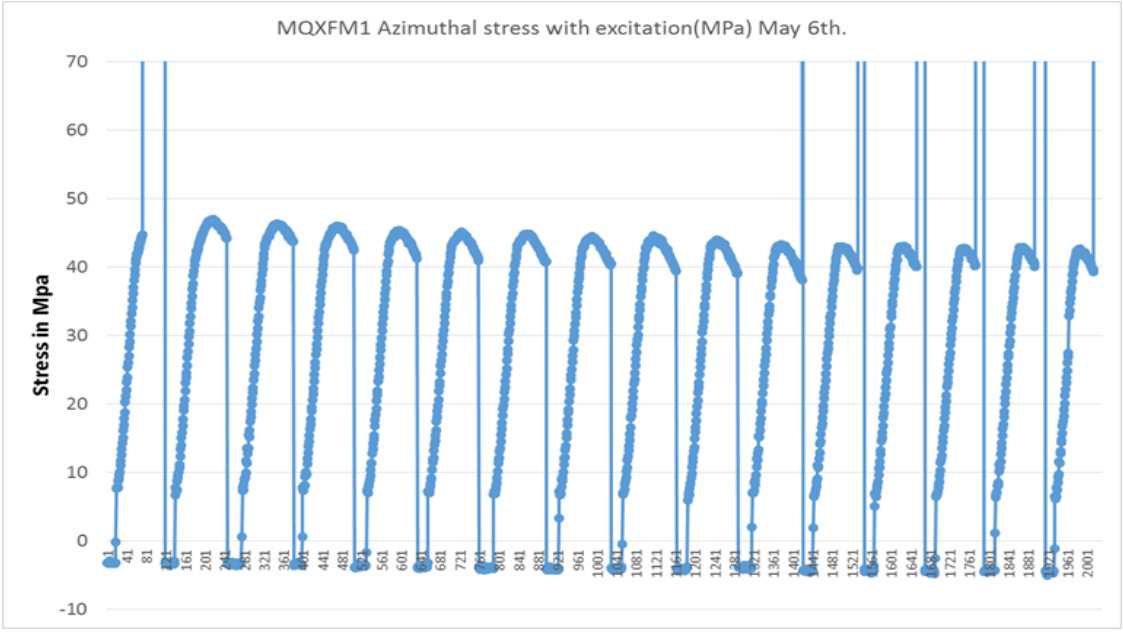

Fig. 27 Azimuthal Stress Subsequent Quenches

Axial full bridges show the strain decreasing from +250 µS to -250 µS during cooldown as shown in Fig. 28. There is a slight tensile strain increase with current, returning at quench, as shown in Figures 29 and 30. This is typical of axial bridges in mirrors.

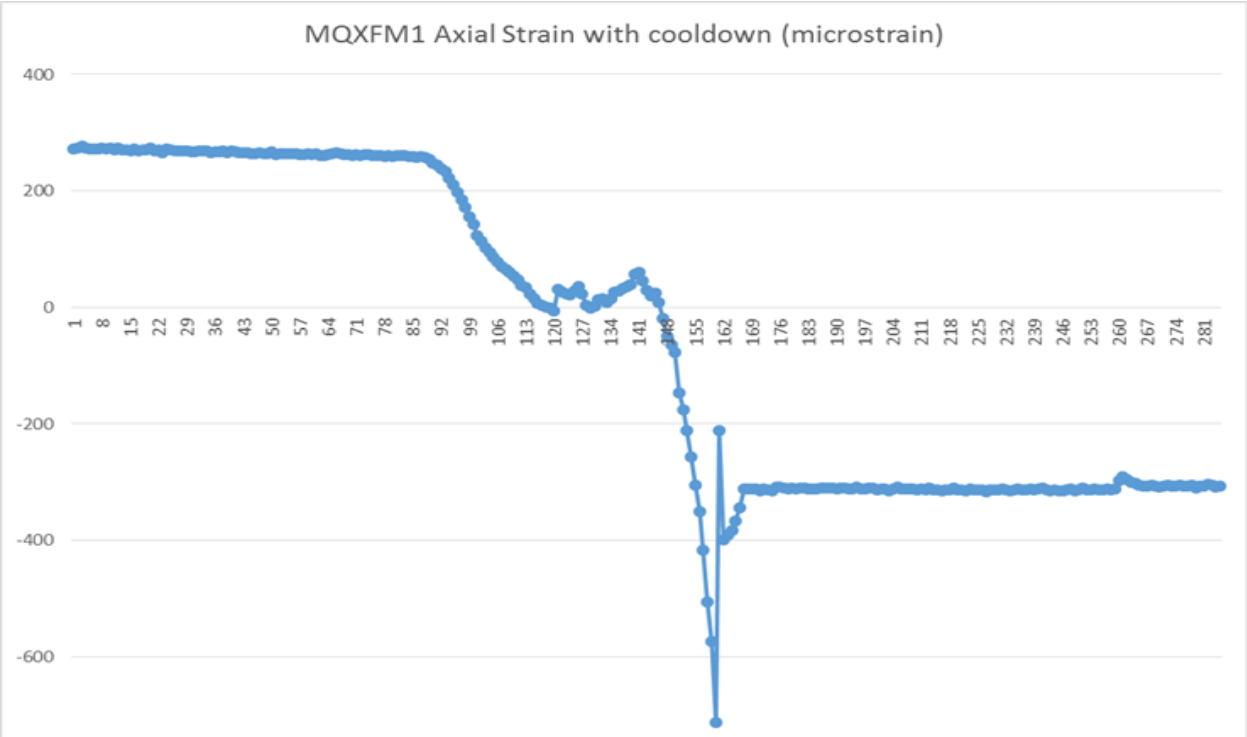

Figure 28 – Axial Strain with Cooldown

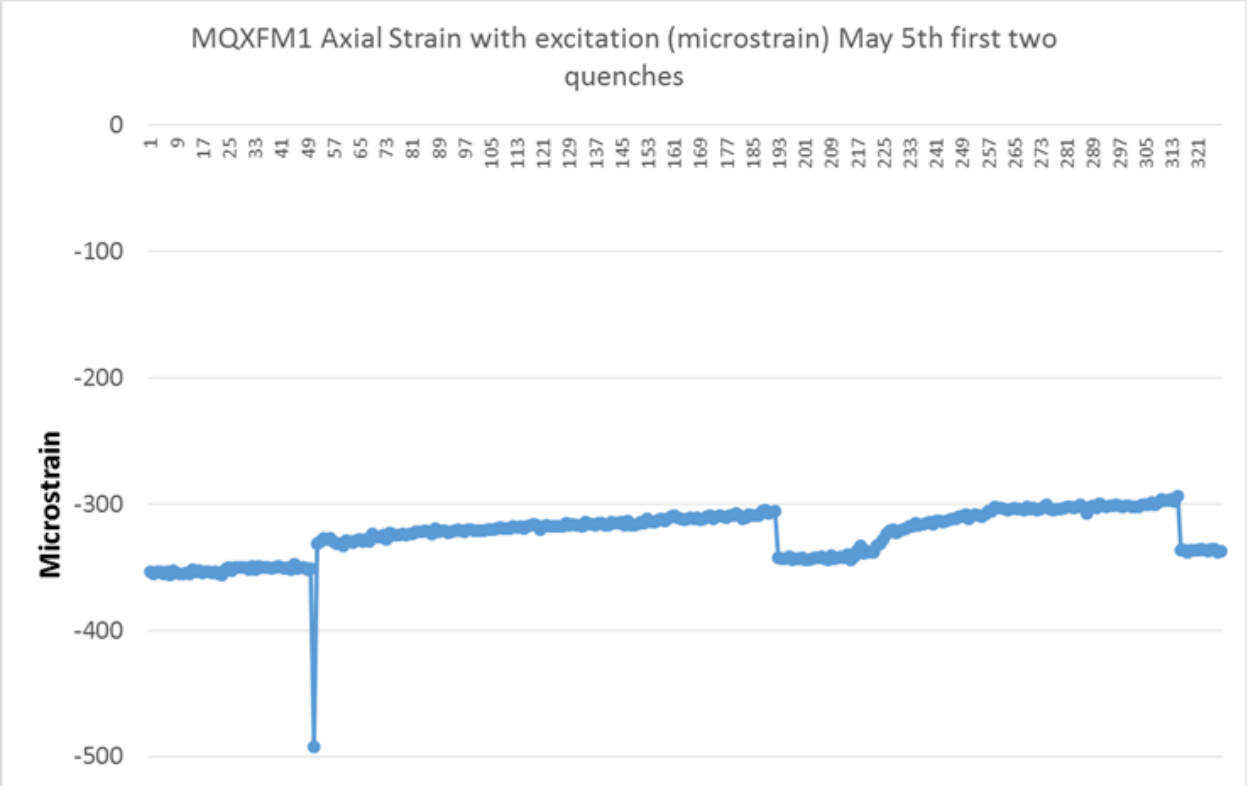

Figure 29 – Axial Strain First Two Quenches

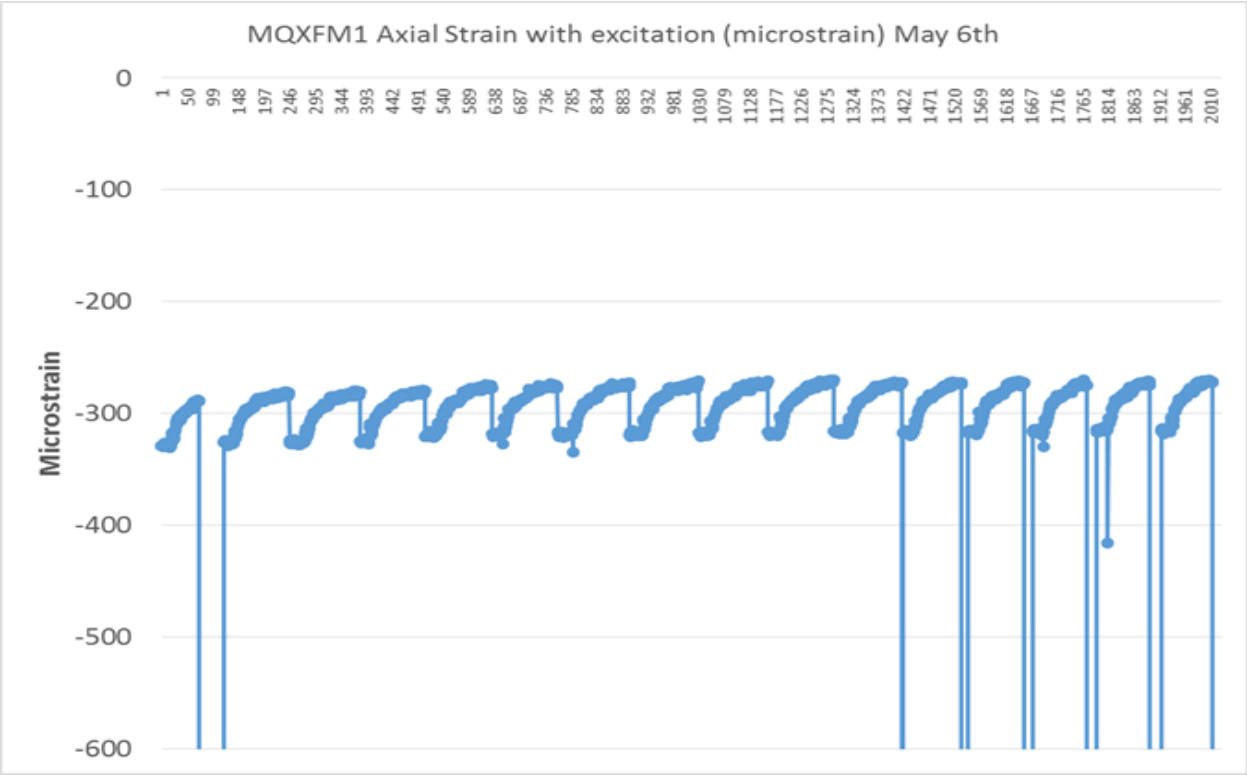

Fig. 30 Axial Strain Subsequent Quenches

Table 2 shows a summary of the strain gauge readings after construction, during and after testing. Note that the azimuthal preload and the axial strain on the titanium bridges have both increased at 290K after testing.

Gauges bonded to the coil are not used during testing, but can be read at 290K before and after testing. Gauges bonded near the midplane also show an increase of preload after testing, indicating that the coil has undergone some permanent deformation in this area. No significant change was noted in the gauges bonded near the pole.

Table 2 – Summary of Azimuthal and Axial Preload

	At 290K after construction	At 4K before excitation	At 1.9K before excitation	Increase with current	At 290K after testing still in structure
Azimuthal Full Bridge (MPa)	-77	-----	-----	+50	-114
Axial Full Bridge (µS)	+270	-300	-350	+50	+500
Coil gauges near pole	-83				-83
Coil gauges near midplane	-72				-91

End preload bolts (bullets) were also read during construction and while testing. Data during cooldown and excitation of the uncalibrated bullets is shown in Figures 31 through 33. Table 3 shows the data when calibration is applied. The value change during cooldown was again unclear. Compressive load increased with current, between 3-7 kN, slightly higher on the return end than on the lead end. Total force on bullet was increased slightly at 290K after testing.

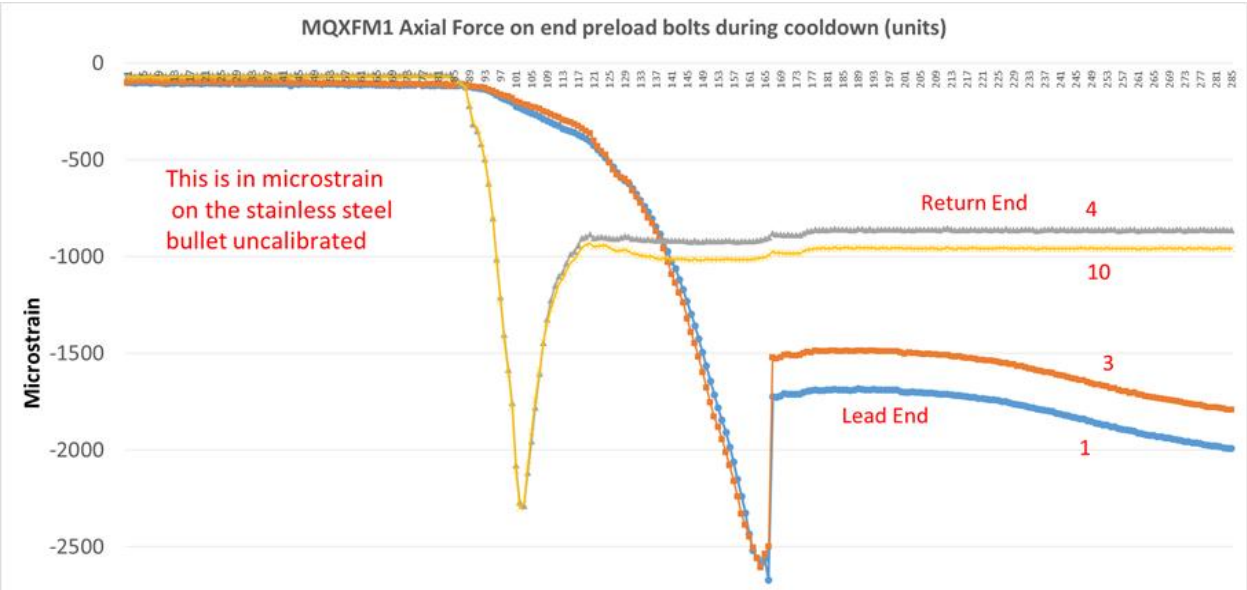

Fig. 31 End Loading with Cooldown

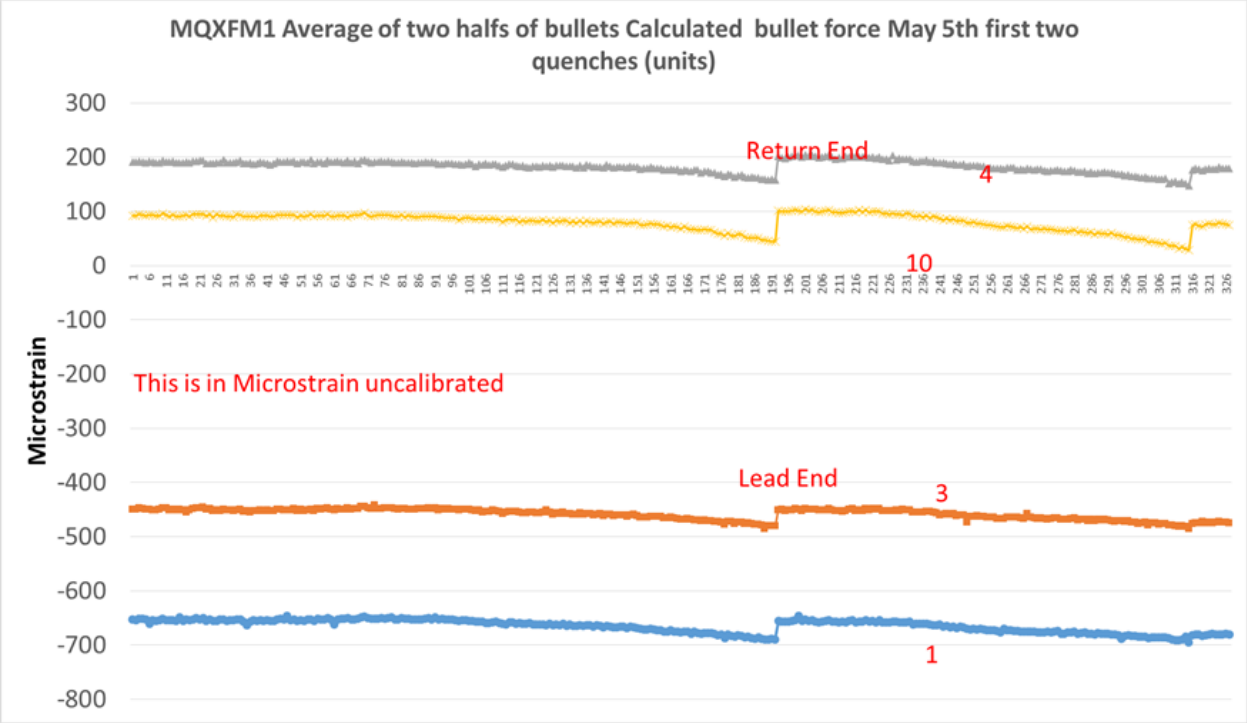

Fig. 32 End Loading First Two Quenches

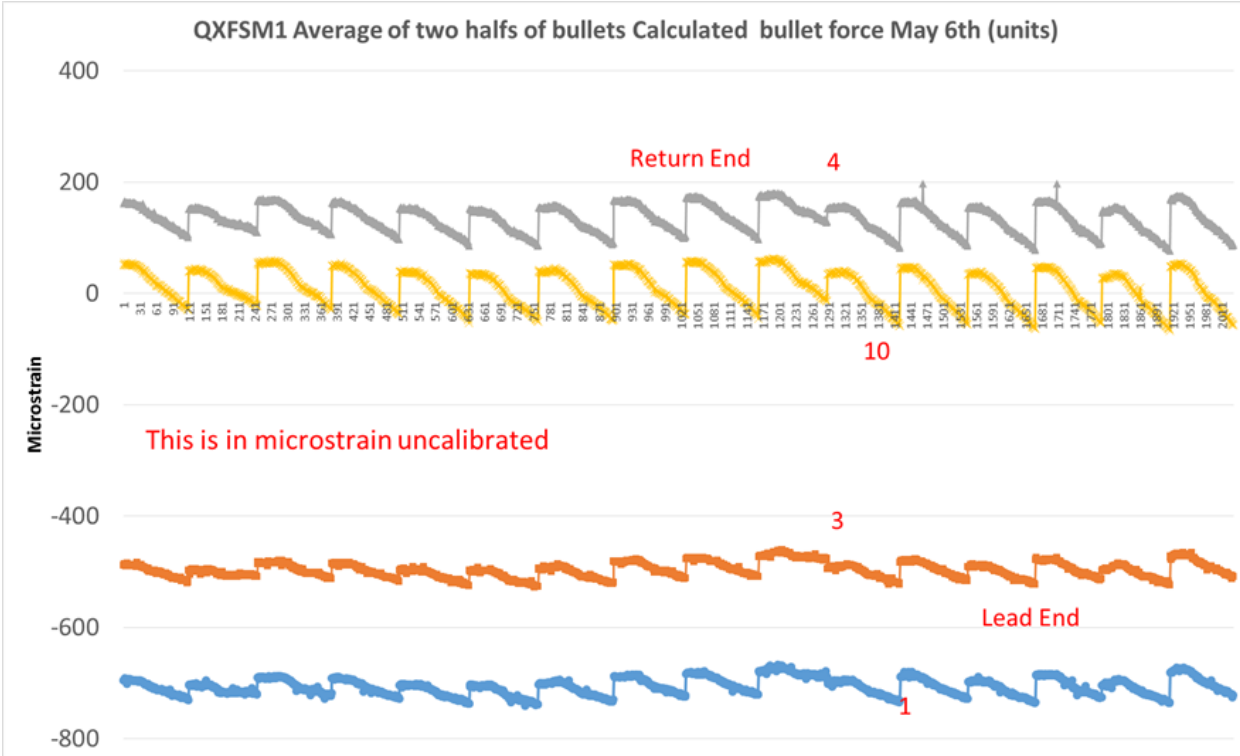

Fig. 33 End Loading Subsequent Quenches

Table 3. - End preload bolt (bullet) readings (units are force in kN)

	At 290K after construction	After installation in dewar 290K	After cooldown to 4.2K	After cooldown to 1.9K	1.9K before quench	1.9K after quench	At 290K after testing
Return End	-13	-4	+7	+10	+1	+8	-21
Lead End	-13	-6	-64	-38	-43	-40	-22

9.4. Strain gauge summary

- Azimuthal full bridges – large positive change in strain with cooldown. Typical of some other mirrors. Possibly due to bending of coil. Increase with current of about 50 MPa.
- Axial full bridges – strain from +250 µS to -250 µS with cooldown. Slight tensile strain increase with current, returning at quench. Typical of axial bridges.

- End load “bullets” - Value change with cooldown unclear. Increase in compressive load with current, between 3-7 kN, slightly higher values on Return End than Lead End. Increased total force at 290K after testing.
- Coil gauges – Uncalibrated. Some sign of permanent deformation at midplane.
- Shell gauges not analyzed
- Coil gauges with excitation not analyzed

10. Quench Protection Studies

10.1 Minimum power density to quench

Goal of this test was to find the minimum heater power density needed to quench the magnet. Either the IL or OL heaters were fired gradually increasing the power density while the other heaters were protecting the magnet. The minimum heater power density at different magnet currents is shown in Fig. 34. All power density calculations assume that the heating power is deposited in the stainless steel heating stations. Time constant of the HFU circuit for these tests varied from 40 ms (IL) to 47 ms (OL).

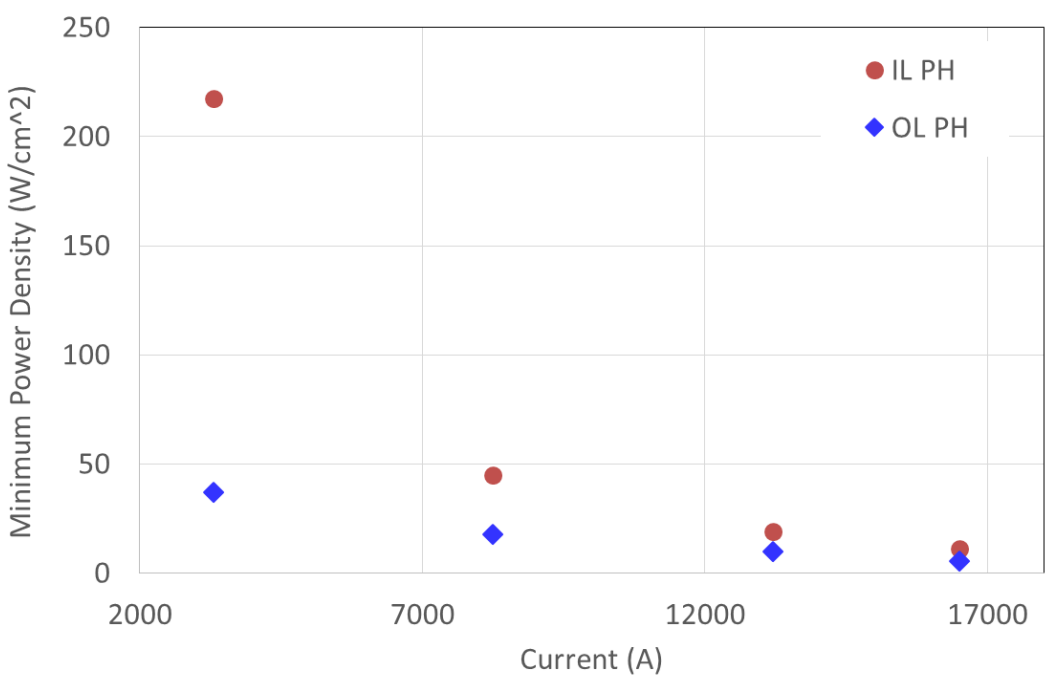

Fig. 34 Minimum heater power density required to quench the magnet at different currents

10.2 Protection heater delays

Protection heater delay time was defined as the time between the heater ignition and the start of quench development in the magnet. For every test a pair of the IL or OL heaters were fired while another pair of heaters were used for the magnet protection, along with the stored energy extraction system. The dump delay was set to 3 ms in order to see the quench development after its detection.

IL and OL heater delays at different magnet currents and for different peak power density are shown in Fig. 35 and 36. Decay time constant for the IL heaters was 40.5 ms, while for the OL midplane and pole heaters (see Fig. 3) it was 94.5 ms and 92.7 ms respectively.

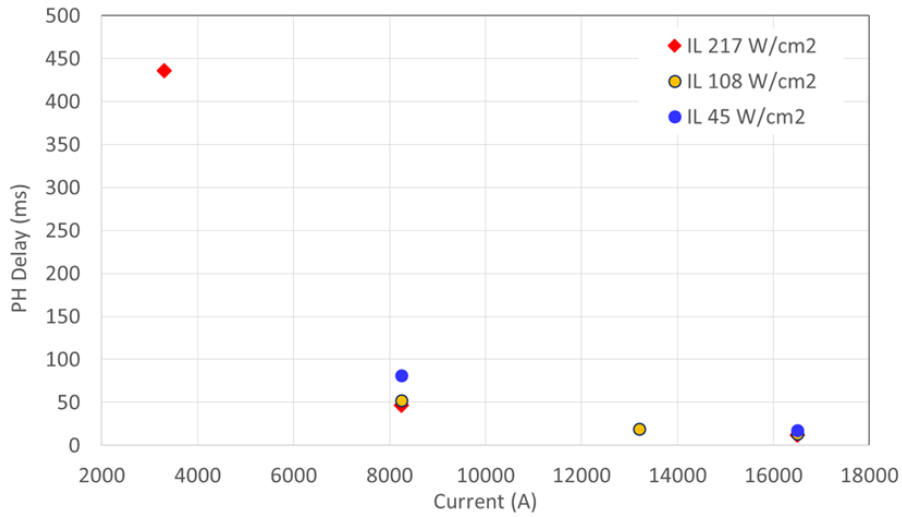

Fig. 35 IL heater delay at different currents

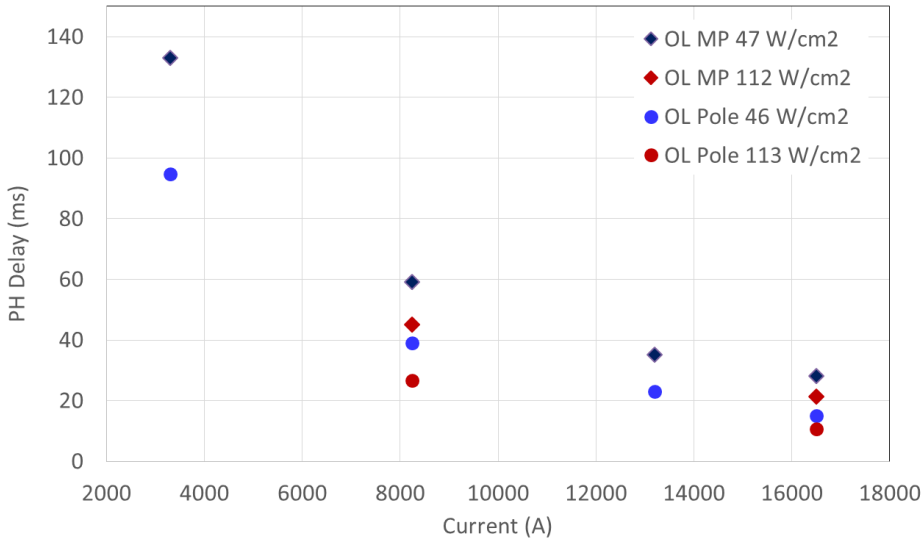

Fig. 36 OL heater delay at different currents

PH delay as a function of the peak power density is shown in Fig. 37. These tests were performed at 8.2 kA and 16.5 kA currents corresponding to 40% and 80% of SSL respectively.

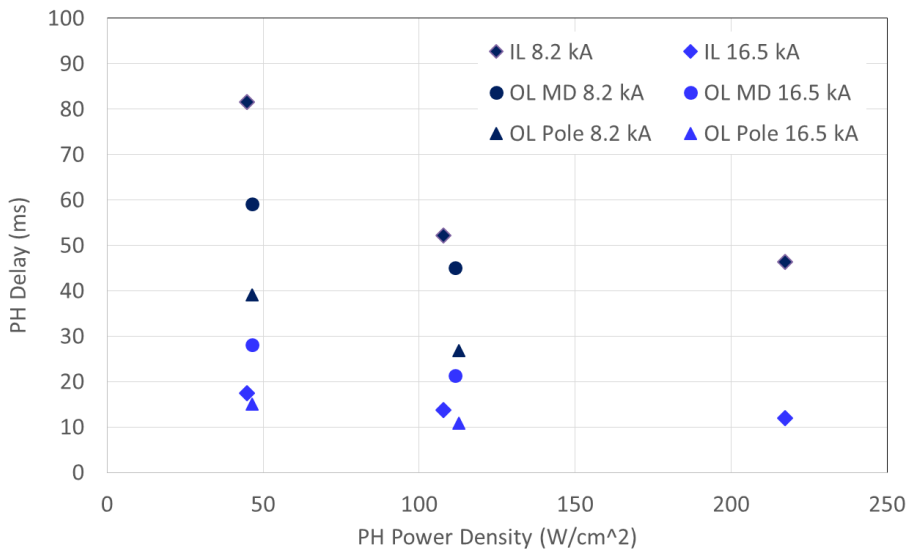

Fig. 37 PH delay vs peak power density

We also investigated the PH delay vs the decay time constant (τ=RC) which was adjusted by changing the heater firing unit (HFU) capacitance. The results of these tests are shown in Fig. 38.

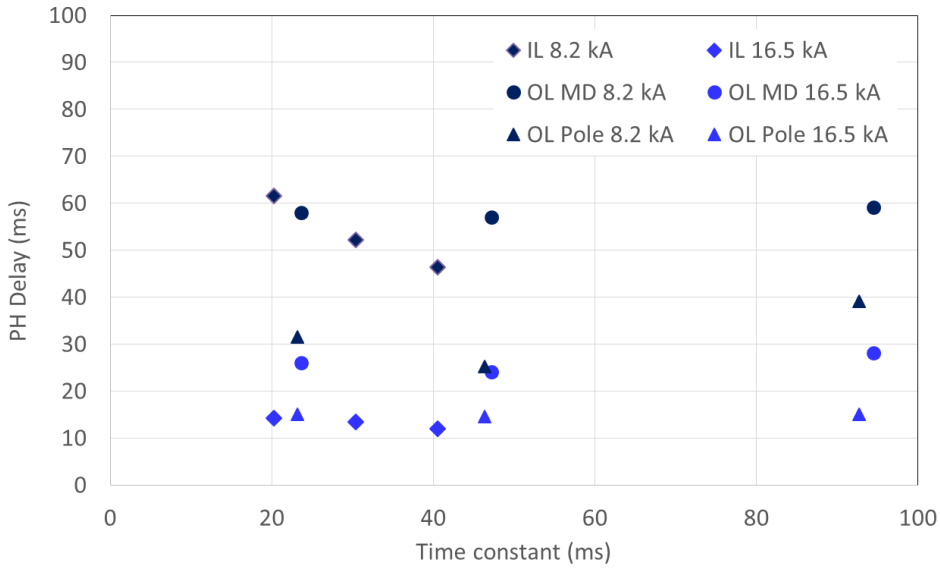

Fig. 38 PH delay vs decay time constant

Finally we investigated reproducibility of heater tests. Both the IL and OL (midplane and pole heaters connected in parallel) heaters were tested 3 times at 11.7 kA and the nominal peak power density of ~50 W/cm^2. The magnet was held at the current flat top for 2 minutes before inducing the heater quench, see test results in Tab. 4.

Table 4

	Test 1, PH delay (ms)	Test 2, PH delay (ms)	Test 3, PH delay (ms)
IL	25.7	28.4	25.9
OL	24.6	25.2	25.9

10.3 Quench Integral study

The quench integral (QI) is determined by integrating $I^2(t)$ over the time and is measured in $10^6 A^2 s$ or MIITs. The goal of this study was to measure quench integral (QI) as a function of current for the OL heater induced quenches and without the energy extraction through the dump resistor. Therefore QI was measured with the dump delayed for 1000 ms, which is equivalent to the no-dump or very small dump (~1 mOhm) operation, and with the IL heaters disabled.

At a given current the quench detection system was manually tripped to fire the OL heaters and induce the quench. The quench development time tq in this case is the heater delay time described in previous subsections. Magnet current was gradually increased to experimentally verify the QI dependence on the current and safely approach the MIITs limit.

QI as a function of the magnet current is shown in Fig. 39. Although the QI (t>0) is not directly relevant to the case of an induced quench, it can be used to estimate the MIITs that will be accumulated in a spontaneous quench without the extraction dump. Such an estimate is obtained by adding the decay QI and the MIITs corresponding to the quench detection time at a specific quench current.

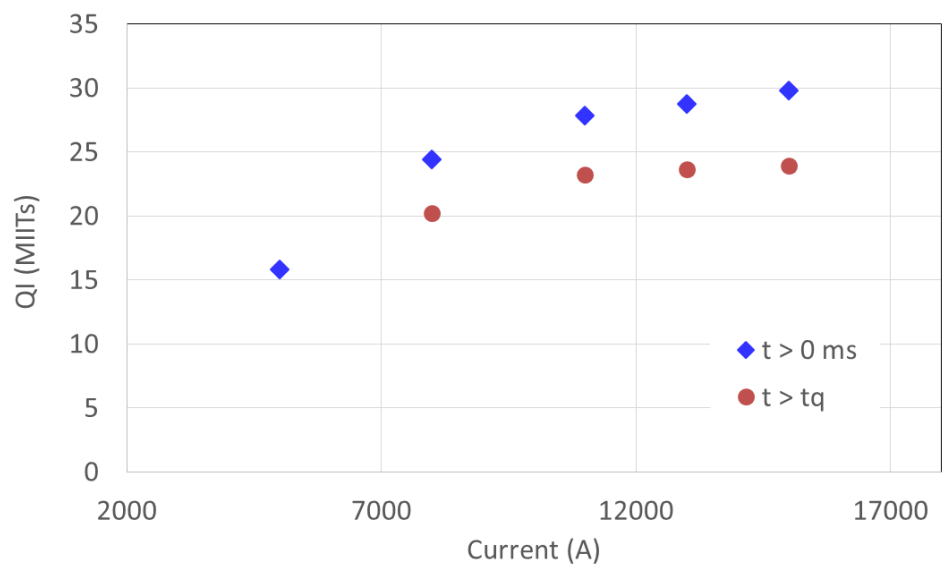

Fig. 39 PH delay vs decay time constant

11. RRR measurements

Estimates of RRR in MQXFSM1 coil segments were made using data captured during the warm up after the test. The warm up was started on May 22nd and transition from superconducting to normal occurred at about 15:48 pm of the same. Data captured at 16:05 pm of May 22nd was used for the cold RRR measurement. Temperature of the magnet bottom was 17.3 K. RTD temperature sensor at the magnet top was lost during the cold test.

Coil voltages across "fixed" and "configurable" voltage tap segments were monitored by the *Pentek* data loggers, while a current of alternating polarity up to +/-10 A, was put through the magnet. For both the warm (~ 300 K) and cold (~ 18 K) measurements we used the RRR amplifier gains for the voltage tap segments to maximize the signal levels.
The magnet reached room temperature and warm voltage measurements were captured on June 1st 2015. Data for all segments, as well as for the whole and half – coils are shown in Fig. 40. Segments around the splices are not shown in the figure.

RRR values for both the configurable and fixed voltage tap segments are reasonably consistent. In average RRR for most of the segments is about 150.

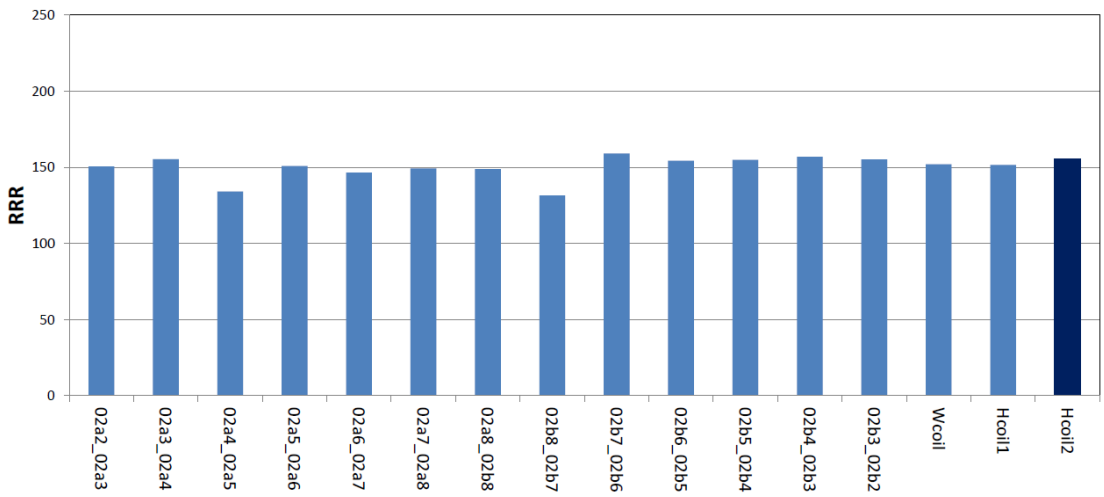

Fig. 40 RRR of MQXFSM1 segments

12. Summary

The first 150-mm aperture Nb_3Sn quadrupole coil was assembled and successfully tested in a mirror structure at Fermilab. The maximum quench current of 19236 A was reached, which corresponds to 91.3% of SSL at 1.9 K. The temperature dependence study of the quench current demonstrated similar magnet performance at all temperatures.

The magnet was held at 16.5 kA or 88% of SSL at 4.5K for about two hours without quenching. MQXFSM1 ramp rate dependence is consistent with the performance of other magnets with a stainless steel core in the conductor.

Average measured RRR was about 150

References

1. E.Todesco et al., "Design Studies of the low-beta quadrupoles for the High-Lumi LHC upgrade", *IEEE Trans. Appl. Supercond., #4002405, issue 3, June 2013*
2. G. Ambrosio, et al., "Final Development and Test Preparation of the First 3.7 m Long Nb_3Sn Quadrupole by LARP", *IEEE Trans. Appl. Supercond.,vol.20, issue 3, pp. 283-287*
3. G. Chlachidze et al., "Performance of HQ02, an Optimized Version of the 120 mm Nb3Sn LARP Quadrupole", *IEEE Trans. Appl. Supercond. Vol. 24, no. 3, June 2014*
   S. Caspi et al., "Test Results of 15 T Nb3Sn Quadrupole Magnet HQ01 with a 120 mm Bore for the LHC Luminosity Upgrade", *IEEE Trans. Appl. Supercond. Vol. 21, no. 3, June 2011*
4. S. Hong et al., "Latest improvements of current carrying capability of niobium tin and its magnet applications", IEEE Trans. on Applied Superconductivity, Vol. 16, Issue 2, 2005, p. 1146
5. D.R. Chichili et al., "Design, fabrication and testing of Nb_3Sn shell type coils in mirror magnet configuration," Adv. Cryog. Eng., 49A, 2004, p. 775.
6. N. Andreev et al, "Magnetic Mirror Structure for Testing Shell-type Quadrupole Coils", *IEEE Trans. Appl. Supercond, vol. 20, issue 3, pp. 288-291*

Attachment I

FPGA (current dependent) Quench Detection (Half-coil signal) thresholds:

1	0-400 A:	0.8 V
2	400-1500 A:	2.0 V
3	1500-3000 A:	2.5 V
4	3000-4000 A:	3.0 V
5	4000-5000 A:	2.5 V
6	5000-6000 A:	2.0 V
7	6000-8000 A:	1.5 V
8	8000-20000 A:	0.8 V

VME AQD Quench Detection (Half-coil signal) thresholds:

0-500 A:	0.8 V
500-6000 A:	2.5 V
6000-15000 A:	0.8 V